Progress In Electromagnetics Research, Vol. 160, 71–87, 2017

Wideband Aperture Coupled Patch Array Antennas — High Gain, Low Side Lobe Design

Dhruva Poduval and Mohammod Ali*

Abstract—The study and design of a wideband aperture coupled microstrip patch array is presented. The proposed design considers the 2.4 to 3 GHz frequency range but may be adapted to other frequencies. A 16 element planar array of the size of about 400 mm by 400 mm by 12.5 mm provides measured gain from 15.4 to 16.8 dBi and Side-Lobe Level (SLL) from 15.3 to 20.7 dB without a reflector within the 2.4 to 3 GHz frequency range. With a reflector significant increase in F/B is obtained but at the expense of higher SLL.

1. INTRODUCTION

Low profile printed antenna arrays with wide bandwidth, high gain, and low SLL are in great demand for current and future commercial and military communication systems and radar. Microstrip patch antennas [1, 2] are excellent candidates for low profile applications. For wideband performance E-shaped and U-shaped slots on microstrip patches have been proposed [3–8]. Stacked patch antennas have also been proposed for moderately wide bandwidth where two patches are coupled to each other to obtain a contiguous dual-band performance [9, 10]. In terms of obtaining wide bandwidth through feeding, aperture coupling is an attractive solution. Aperture coupled patch antennas [11, 12] are preferred particularly for phased arrays because of their advantage of integration to other active devices and circuits, e.g., phase shifters, power amplifiers, low noise amplifiers, mixers etc. However, when designing such arrays, the interplay between array performance characteristics, such as gain, SLL, back lobe level, mutual coupling etc. must be understood and optimized under multiple design constraints, e.g., substrate material properties and thicknesses, element to element spacing, and feed lines and their orientation and arrangements with respect to the antenna elements. In the literature there are many examples of aperture coupled patch antenna element design but not so much on array design, especially high gain, low side lobe, and low back lobe array design. The focus of this paper is to investigate, design, and develop an aperture coupled patch array with wide operating bandwidth (30%), high gain (17.5 dBi), low SLL (20 dB), and high Forward to Backward (F/B) ratio (21.8 dB). The frequency range targeted here is the 2.4 to 3 GHz frequency band because of its wide application in WLAN, LTE (Long Term Evolution) and other communication systems. Notwithstanding that the design concept can very well be adapted at other frequencies. Preliminary work on the proposed concept was recently introduced in our conference paper [13]. The current paper goes much beyond that.

Specifically, a 16 element, 4 by 4 planar microstrip patch array is designed using HFSS and experimentally developed and tested. Starting from mutual coupling minimization a corporate feeding scheme is designed to achieve the needed performance. To reduce the SLL the corporate feeding network is redesigned to obtain a specific amplitude taper. Studies are conducted to determine the optimum location for a metallic reflector under the feed line to improve the F/B. An experimental prototype of the array was built and tested validating and demonstrating the performance levels expected from simulation predictions.

Received 29 September 2017, Accepted 17 November 2017, Scheduled 8 December 2017

* Corresponding author: Mohammod Ali (alimo@cec.sc.edu).
The authors are with the Department of Electrical Engineering, University of South Carolina, 301 Main Street, Columbia, SC 29208, USA.

2. THE ANTENNA ELEMENT

An aperture coupled patch antenna shown in Fig. 1(a) was considered as the element of choice to design and build the proposed array because of its wide bandwidth potential and ease of integration with other RF circuits. The feedline being on the bottom allows easier integration with other RF circuits, e.g., phase shifters, power amplifiers etc.. For both the antenna and feed substrates RO4003C was considered. Rohacell was chosen to be the foam substrate for use between the antenna and the feed substrates.

Simulations of the antenna were conducted using HFSS. The patch size, substrate thickness, slot dimensions, and the microstrip stub dimensions were optimized to meet the desired bandwidth. All dimensions are listed in Table 1. The sensitivity of the stub length, l_{oc} on antenna impedance matching

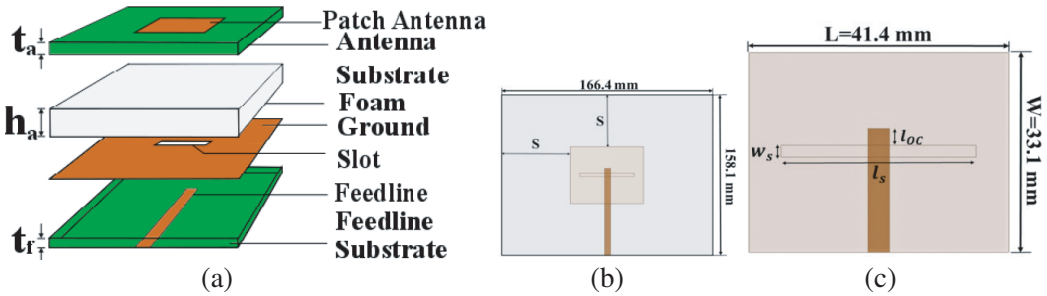

Figure 1. (a) Aperture coupled patch stack-up, (b) substrate size and patch location, (c) patch, slot, and stub dimensions.

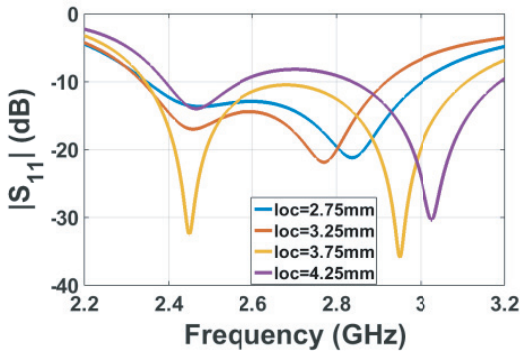

Figure 2. Simulated S_{11} vs frequency with the stub length, l_{oc} as the parameter.

Table 1. Optimized dimensions of the aperture coupled patch, its substrates, and feedlines for 2.4 to 3 GHz operation. Patch and feed substrate is RO4003C; foam is Rohacell foam.

Parameter	Dimensions (mm)
Patch length, L	33.1
Patch width, W	44.1
Antenna Substrate Thickness, t_a	1
Feedline Substrate Thickness, t_f	1.52
Foam thickness, h_a	10
Stub length, l_{oc}	3.75
Slot length, l_s	31
Slot width, w_s	2

with reference to a 50 Ω feed impedance is shown in Fig. 2. As seen, the antenna operates within the 2.4 to 3 GHz frequency band within $|S_{11}| \leq -10$ dB for $l_{oc} = 3.75$ mm. It is clear that selecting an optimum l_{oc} is important to obtain a good S_{11} performance. Radiation patterns and gain of the antenna were also computed but are not shown here for brevity.

3. LINEAR ARRAY OF APERTURE COUPLED PATCHES

Before proceeding with the design of a planar m by n corporate-fed patch array with appropriate amplitude taper studies were conducted in a step by step manner to reduce design risks. First, a four-element linear patch array shown in Fig. 3 was analyzed. In Fig. 3 each element of the array is individually fed using its own separate feedline. Each patch is excited with the same amplitude and phase. The inter-element separation chosen was $d = 62.5$ mm which is 0.5λ at 2.45 GHz. Simulated selected S-parameters of the array are shown plotted in Fig. 4. As seen from the plots, the array has an operating bandwidth from 2.36 to 3.18 GHz (29.6%). Mutual coupling (S_{mn}) results show that the strongest mutual coupling (−15 dB)occurs between adjacent elements as expected.

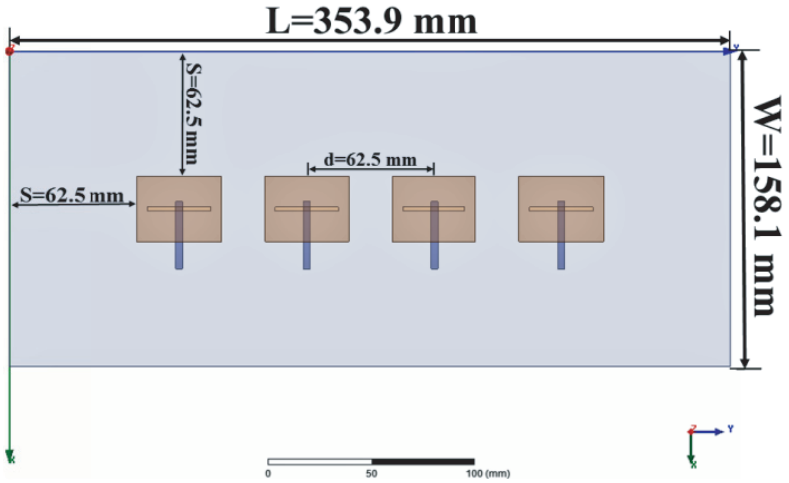

Figure 3. Four element aperture coupled patch array, separately excited.

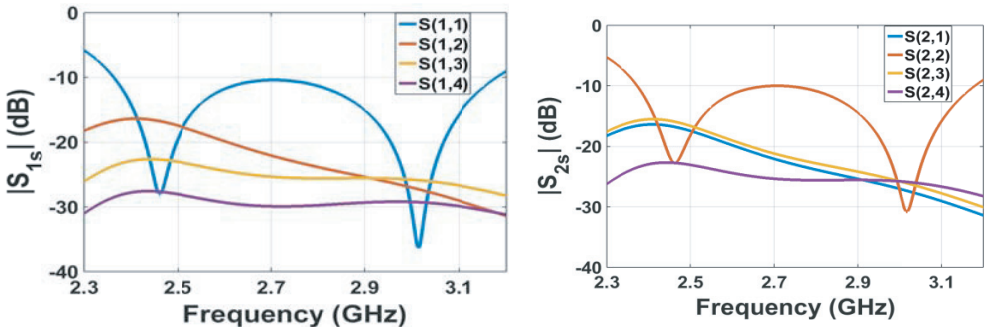

Figure 4. Simulated S-parameters of the 4-element patch array.

4. PLANAR ARRAY

4.1. Separately Excited 4 × 4 Planar Patch Array

A 16-element, 4 by 4 planar array can be viewed as an array of 4, 4 element linear array antenna. The center to center inter-element separation between two adjacent elements in the antenna is kept at

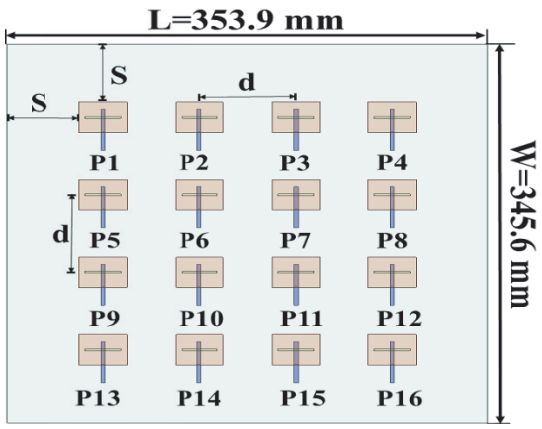

Figure 5. Sixteen element array, separately excited.

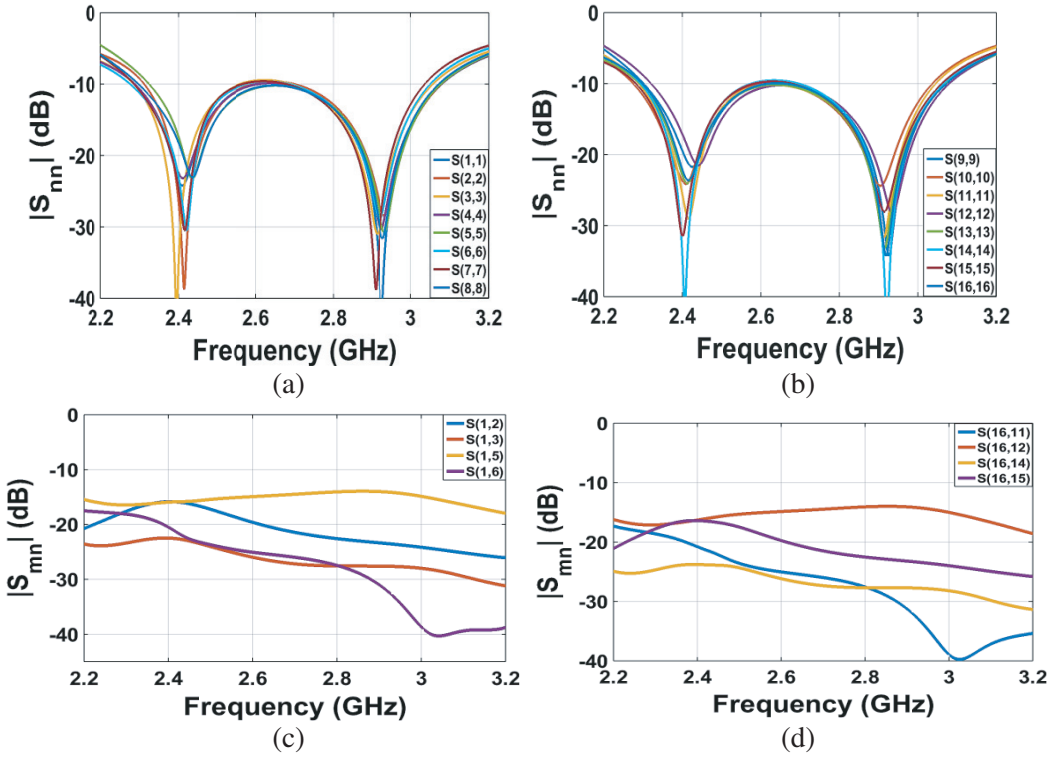

Figure 6. Simulated S_{nn} and S_{mn} parameters vs frequency for the 16 element array.

$d = 62.5$ mm. The top view of this 4 by 4 planar array can be seen in Fig. 5.

As before, each antenna element is individually excited using its own feedline. All 16 ports, P1 through P16 are labelled in Fig. 5. Simulated S-parameter results for this array are shown in Fig. 6 for selected cases. The S_{nn} data show that each antenna is operating from about 2.3 to 3.05 GHz. Comparing these results with the S_{nn} results shown in Fig. 4 the latter data show signs of slight deterioration in the impedance matching. The bandwidth has also reduced slightly at least at the upper edge of the band. The mutual coupling data, S_{mn} for some of the important cases are plotted in Fig. 6. Strong mutual coupling (-13 dB) is observed between elements $(1, 5)$, $(6, 2)$, $(6, 10)$, $(16, 12)$ etc.. It is clear that these elements are arranged along the E-planes of the patches and hence see stronger coupling [14]. Simulated radiation patterns for this array are plotted in Fig. 7. As seen, patterns are directional with one well-defined beam, 2 or more side lobes and 2 or more back lobes. A summary of

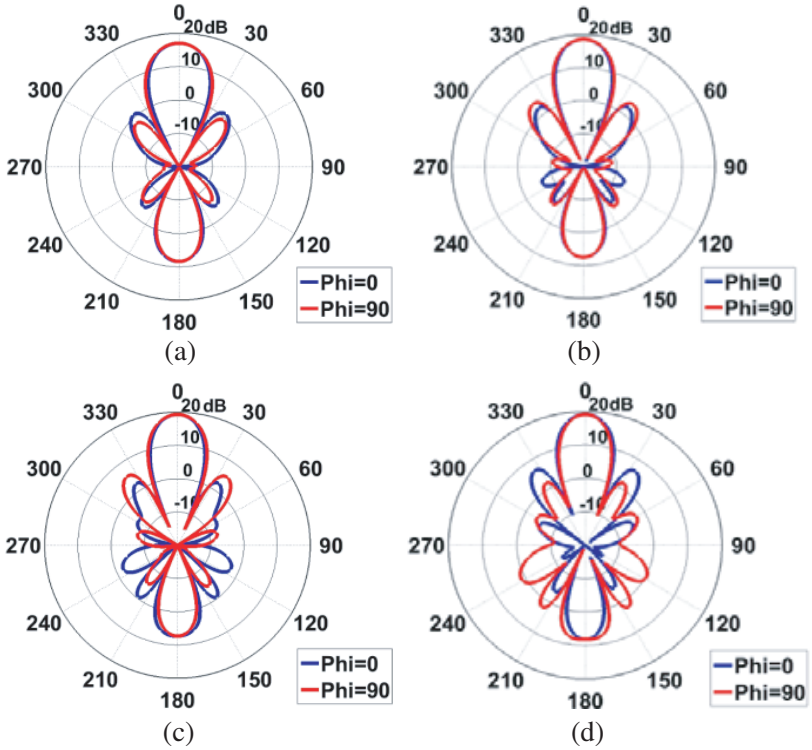

Figure 7. Simulated radiation patterns at (a) 2.45, (b) 2.65. (c) 2.85, and (d) 3.05 GHz.

Table 2. Summary of simulation results for individually fed planar array antenna.

Frequency (GHz)	Realized Gain (dBi)	SLL (dB)	F/B (dB)
2.45	17.0	16.3	8.6
2.65	18.7	14.3	11.2
2.85	19.3	14	12.0
3.05	19.1	12.6	11.0

the simulated pattern parameters are listed in Table 2. Gain is from 17 to 19.3 dBi, SLL from 12.6 to 16.3 dB, and F/B from 8.6 to 12 dB.

4.2. Corporate Fed 4×4 Planar Patch Array

4.2.1. Initial Results

The 16 element planar array was then excited using a corporate feeding network shown in Fig. 8(a). Quarter wave matching sections were used to match two 50 Ω lines in parallel. The impedance of the quarter wave section was calculated as [15]

$$Z_{\lambda/4} = \sqrt{Z_L Z_0} \tag{1}$$

where $Z_L = 50 \| 50 = 25\,\Omega$ and $Z_0 = 50\,\Omega$ giving $Z_{\lambda/4} = 35.4\Omega$.

The width of the 50 Ω line and the quarter wave matching sections were $w_1 = 3.5$ mm and $w_2 = 5.8$ mm, respectively. The length of the quarter wave section was calculated using [15] Eqs. (2) and (3)

$$\lambda = \frac{c}{f\sqrt{\varepsilon_{eff}}} \tag{2}$$

$$\varepsilon_{eff} = \frac{\varepsilon_r + 1}{2} + \frac{\varepsilon_r - 1}{2} \frac{1}{\sqrt{1 + \frac{12\, t_f}{w_2}}} \tag{3}$$

where $c = 3 \times 10^8$ m/s and $t_f = 1.52$ mm.

The length of each quarter wave section was 18.26 mm considering 2.45 GHz as the design frequency.

Simulated S_{11} data of the corporate fed array are shown plotted in Fig. 8(b). It is clear that the array impedance matching has significantly deteriorated compared to the separately fed 16 element array (see Fig. 6). The bandwidth of the corporate fed array is much narrower (2.6 to 2.96 GHz) than the bandwidth (2.3 to 3.05 GHz) of the individually fed array. By examining the feeding arrangement shown in Fig. 8(a) it is clear that the slots are all excited from the bottom edge of each patch. This creates an asymmetry in the positioning of the feedlines. By "asymmetry" we mean that the feedlines are closer to some primary slots than others. For example, feedline A is closer to elements 11 and 12 than elements 7 and 8. Similar is the situation for feedlines B and C. This prompted us to conduct further investigations of the electric field magnitudes on the slots and the feedlines. Computed electric field magnitudes for the array with $d = 62.5$ mm are shown in Fig. 9(a). The electric field magnitudes reveal that the fields

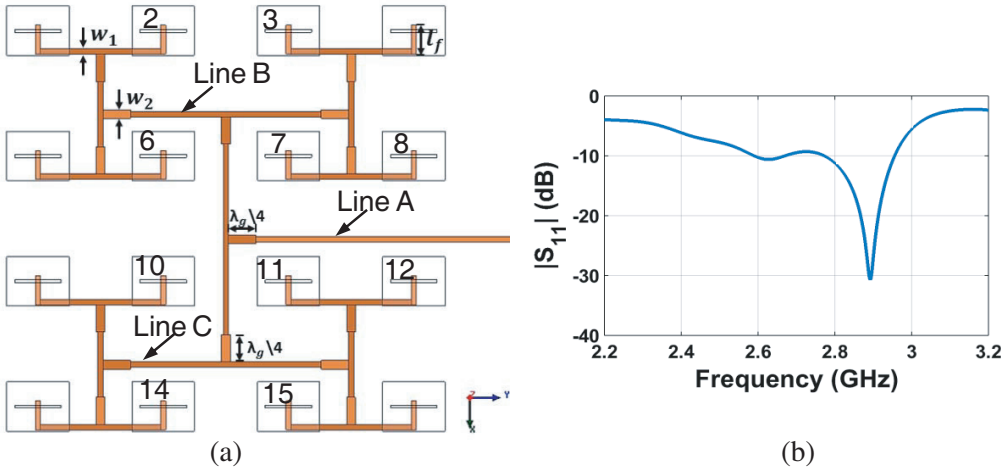

(a) (b)

Figure 8. (a) Corporate fed patch array and (b) simulated S_{11} vs frequency.

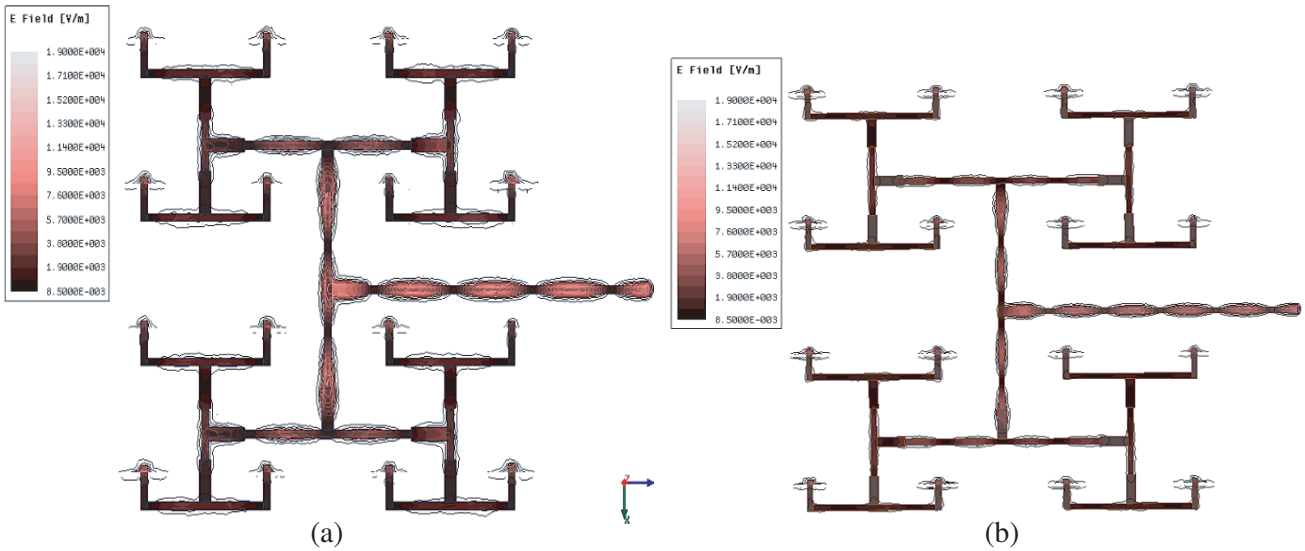

(a) (b)

Figure 9. Magnitude of E-fields for (a) $d = 62.5$ mm and (b) $d = 83.3$ mm.

reaching the slots are quite weak, uneven between the slots and degraded. The other significant issue observed was the rather strong mutual coupling (−13 dB) between adjacent elements along the E-plane. These observations prompted us to increase the interelement distance to $d = 83.3$ mm ($2\lambda/3$ at 2.4 GHz) and study the array performance.

4.2.2. Further Analysis

Increasing the distance to $d = 83.3$ mm allowed more distance between the slots and the lines marked A, B, and C in Fig. 8(a). Increasing d increased the overall array size to 416.3 mm by 407.6 mm. Computed E-field magnitudes for this new configuration are shown plotted in Fig. 9(b). It is evident that the E-fields are uniformly distributed across the feedlines and slots for the case with $d = 83.3$ mm.

To fully appreciate the effects of the new interelement distance on array impedance matching and mutual coupling the performance of an individually excited 4 by 4 array with $d = 83.3$ mm was studied before analyzing the array integrated with the corporate feed network. Fig. 10 shows the results of the individually fed array with $d = 83.3$ mm. The S_{nn} have been divided into two plots, the first plot Fig. 10(a) depicts the performance of antennas from port 1 to port 8, whereas Fig. 10(b) shows the reflection coefficient performances seen at ports 9 through 16. The reflection coefficient performances seen for this configuration with an increased inter-element separation is better than the previous design

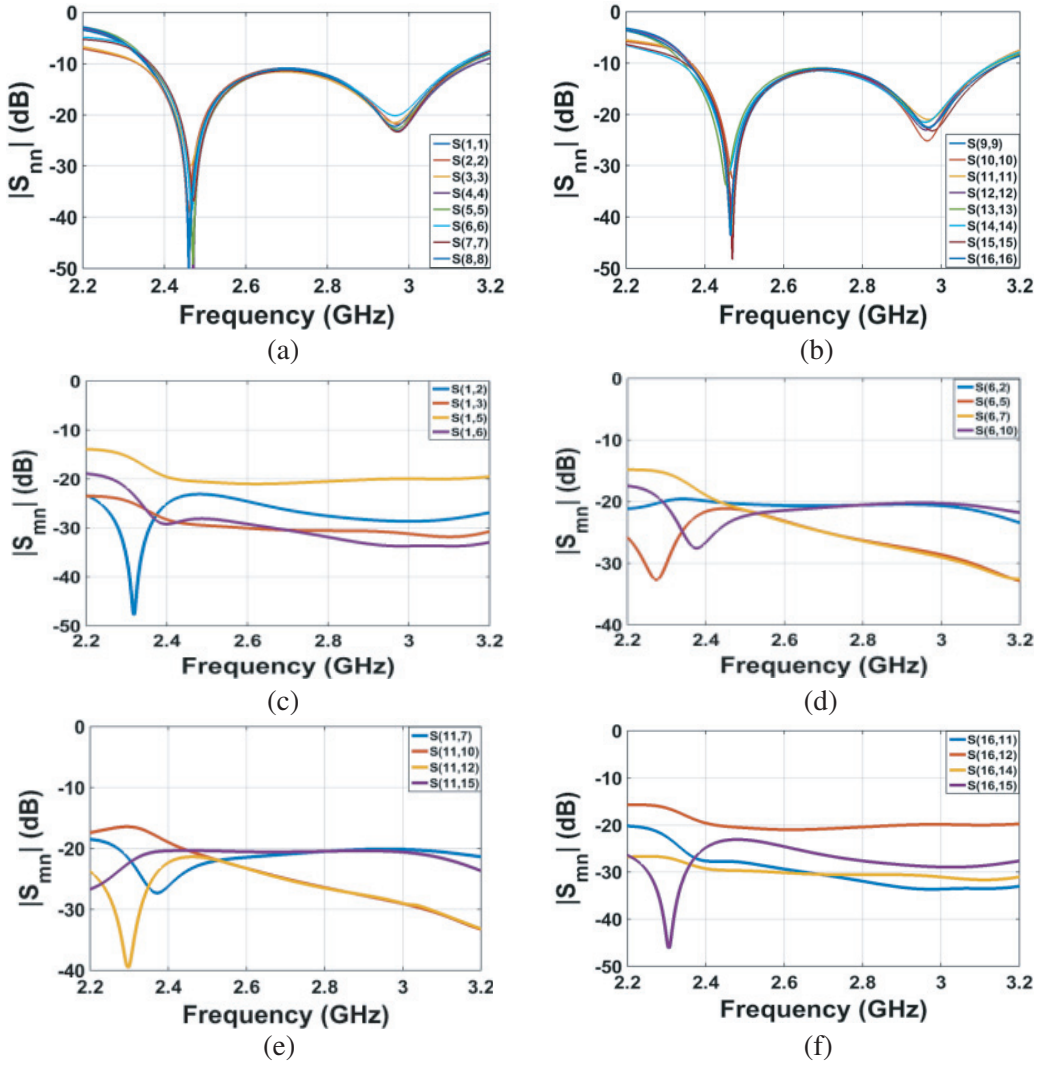

Figure 10. Simulated S_{nn} and S_{mn} for individually fed 16 element array when $d = 83.3$ mm.

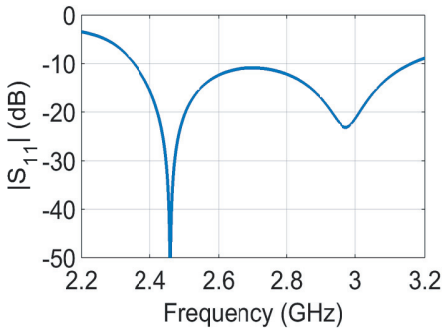

Figure 11. Simulated S_{11} vs frequency for corporate fed array when $d = 83.3$ mm.

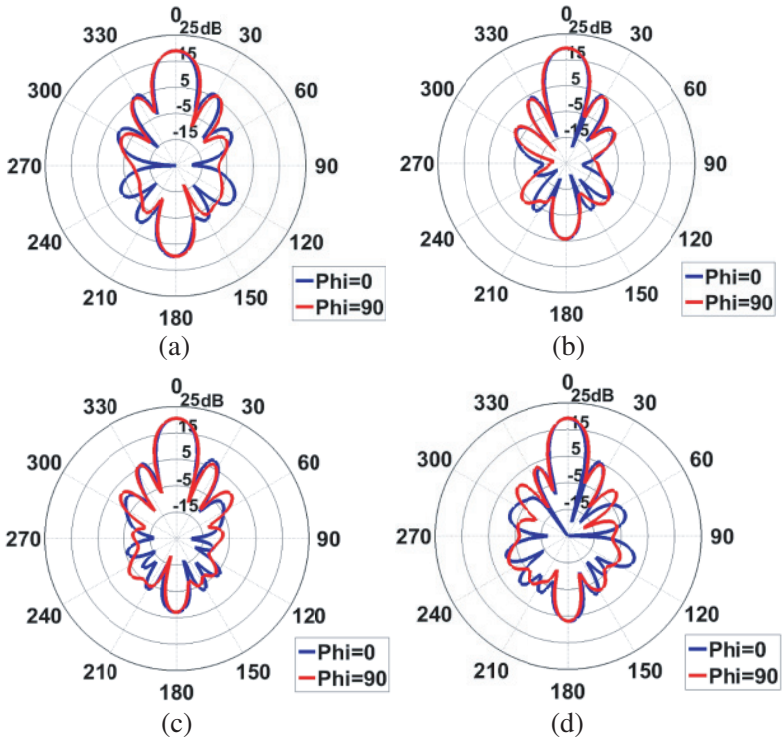

Figure 12. Simulated radiation patterns at (a) 2.45, (b) 2.65, (c) 2.85, and (d) 3.05 GHz.

Table 3. Summary of simulation results for planar array antenna fed using a corporate feed.

Frequency (GHz)	Array Directivity (dBi)	Realized Gain (dBi)	SLL (dB)	F/B (dB)
2.45	19.4	19	12.9	9.3
2.65	20.3	19.5	15.1	15.3
2.85	21.1	20.5	12.7	17.6
3.05	21.3	19.2	15	12.3

across each port. The operating frequency range is still almost the same, lying from 2.3 to 3.1 GHz, but the S_{nn} levels are lower near the design frequency. In the previous design with $d = 62.5$ mm, the S_{nn} within 2.6 to 2.7 GHz exceeded -10 dB (Fig. 6). This problem is resolved now with $d = 83.3$ mm distance (Figs. 10(a) and 10(b)). Selected cases of mutual coupling data versus frequency are plotted in Figs. 10(c)–10(f). Only the cases with moderate to high coupling are shown. Comparing the mutual coupling of Figs. 10(c)–10(f) with those of Figs. 6(c)–6(d) it is clear that the coupling is significantly

lower for the latter case.

Next, the 4 by 4 array was integrated with the corporate feed network with $d = 83.3\,\text{mm}$ interelement distance and simulated. Simulated S_{11} performance of the corporate fed 4 by 4 array is shown in Fig. 11. The array operates from 2.35 to 3.15 GHz. Simulated patterns at several frequencies are shown in Fig. 12. Patterns look directional with realized gain between 19.2 and 20 dBi. Other relevant pattern parameters are summarized in Table 3.

4.3. Corporate Fed Low Side Lobe 4×4 Planar Patch Array

4.3.1. Simulation Results

Following the corporate-fed array design described above a low SLL array design was approached next. This required providing non-uniform excitations to the elements of the array. Modifications to the corporate feed network were made to provide non-uniform excitation to each patch. The excitation coefficients were determined by considering an SLL level of $-25\,\text{dB}$ at 2.45 GHz. For a maximum to minimum of 25 dB in terms of power ratio attention was paid to find transmission line trace widths that were not too narrow which could be difficult to fabricate in our lab. A minimum line width of at least 0.4 mm was considered.

The taper coefficients were calculated based on a technique described in [16, 17]. The obtained power division profile was as follows,

$$\begin{bmatrix} 0.054 & 0.23 & 0.23 & 0.054 \\ 0.23 & 1 & 1 & 0.23 \\ 0.23 & 1 & 1 & 0.23 \\ 0.054 & 0.23 & 0.23 & 0.054 \end{bmatrix}$$

This matrix was generated by employing an iterative Fourier transform technique which generates an array factor for the required SLL. Here each element of the matrix represents the amplitude taper coefficient of the corresponding array element. Fig. 13 shows the corporate feed network which provides the above power distribution. It consists of T-junction power dividers and quarter wave transformer sections used for matching. The various line widths on the corporate feed network are obtained as follows.

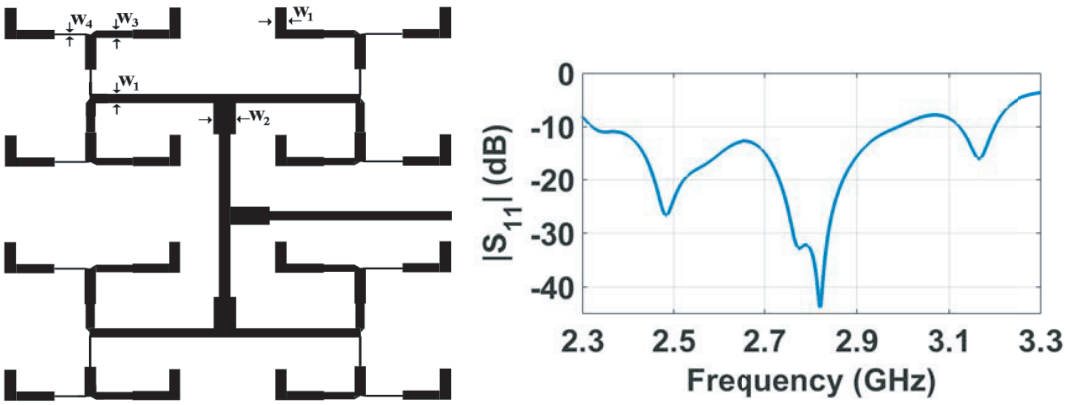

(a) (b)

Figure 13. (a) Amplitude tapered corporate feed, (b) simulated S_{11} performance.

The line with width $w_1 = 3.5\,\text{mm}$ has a characteristic impedance of $50\,\Omega$. Let us say P_{IN} is the power entering the node lying between the arms labelled $w3$ and $w4$. If P_3 and P_4 are the powers flowing in the respective arms, then we can say that,

$$P_{IN} = P_3 + P_4$$

Therefore for an unequal power distribution [16, 17],

$$P_3 = kP_{IN}$$
$$P_4 = (1-k)P_{IN}$$

Therefore, to obtain an impedance match at the terminal the impedances have to be as follows,

$$Z_3 = \frac{Z_1}{k}; \qquad Z_4 = \frac{Z_1}{(1-k)}$$

where Z_3 and Z_4 are the required impedances seen looking in from arms 3 and 4 respectively to obtain a matched network with the desired power division ratio. Therefore, the impedance of the quarter wave transformer sections needed to match the network will be,

$$Z_{w3} = \sqrt{Z_3 Z_1}; \qquad Z_{w4} = \sqrt{Z_4 Z_1}$$

Solving the above equation we get, $w_3 = 2.94\,\text{mm}$, $w_4 = 0.6\,\text{mm}$. The width of the $35.5\,\Omega$ line is $w_2 = 5.8\,\text{mm}$.

Simulated S_{11} results of this array are shown in Fig. 13(b). The S_{11} plot shows that the antenna has an operating bandwidth of (2.32–2.99 GHz and 3.12–3.2 GHz). Simulated radiation patterns are shown in Fig. 14. All radiation performance data are also listed in Table 4. The peak realized gain seen at these four frequencies is between 17.2 and 18.6 dBi. The SLL at the design frequency is 25.5 dB. The SLL drops to about 18.5 dB at the upper end of the operating frequency of the antenna which is to be expected as the taper coefficients were designed for 2.45 GHz.

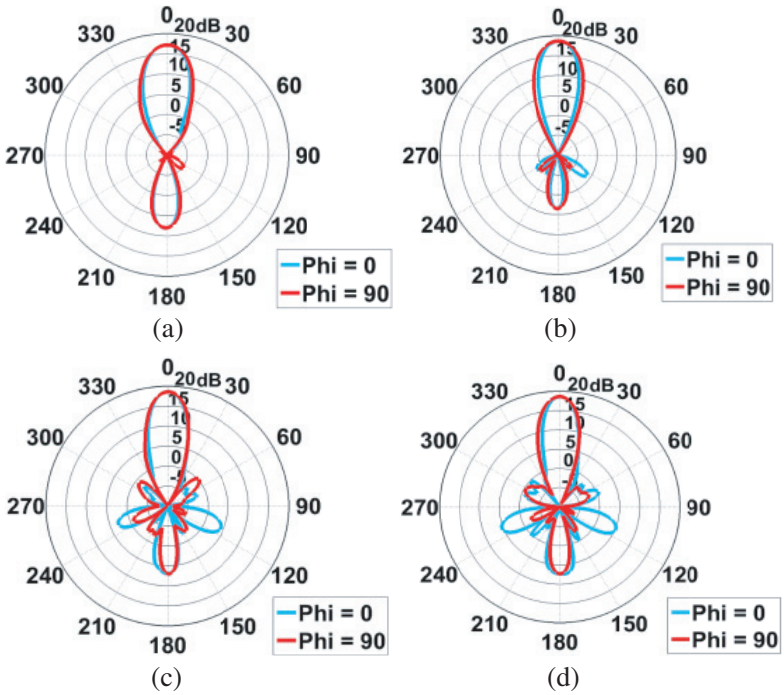

Figure 14. Simulated radiation pattern plots at (a) 2.45, (b) 2.65, (c) 3, (d) 3.1 GHz.

Table 4. Simulation data of tapered corporate fed 4×4 array.

Frequency (GHz)	Directivity (dBi)	Realized Gain (dBi)	SLL (dB)	F/B (dB)
2.45	17.7	17.2	25.5	9.3
2.65	19.3	18.6	27.2	15.2
3	19.7	18.6	18.5	11.7
3.1	20	18.6	18.6	11.3

4.3.2. Experimental Results

The 4 by 4 planar array was fabricated using photo-chemical etching. Since the array was too large (greater than 400 mm or 16 inches) it was not possible for us to fabricate it as a single piece. The UV exposure box and the etching tank available in our lab caused the size limitation. To circumvent this problem the patch and feed substrates each were cut into four separate pieces (photos shown in Fig. 15). To minimize the number of places where feed lines needed to be bridged; the pieces were not all of the same size. Small sections of copper tapes were soldered between disconnected transmission lines to bridge them. The four pieces of patch substrates and the four pieces of feed substrates were joined together as shown in Fig. 15. In between them resided the Rohacell foam. Measured S_{11} results for the array are shown in Fig. 16.

As seen, the fabricated array operates from 2.4 to 3.15 GHz. Only within a small frequency range (from 2.82 GHz to 2.96 GHz) the S_{11} exceeds -10 dB. This deterioration of performance can mainly be attributed to the differences in the widths of the narrowest transmission lines that were fabricated. The lines were supposed to be 0.6 mm wide but in some cases they were overetched and were instead between 0.4 and 0.5 mm in width.

Subsequently, the array patterns and gain were measured in a Satimo anechoic chamber (Fig. 17(a)). Measured radiation pattern results at selected frequencies are shown plotted in Fig. 17(b). As seen, all patterns are highly directional. Pattern related important data are summarized in Table 5. Antenna gain varies from 15.4 to 16.8 dBi while SLL varies from 15.3 to 20.7 dB and F/B varies from 14.7 to 25.4 dB.

The measured realized gain is seen to be about 1.7 to 2.8 dB lower than what the simulations

(a) (b) (c)

Figure 15. (a) Corporate feed, (b) ground plane with slots, (c) top view of array.

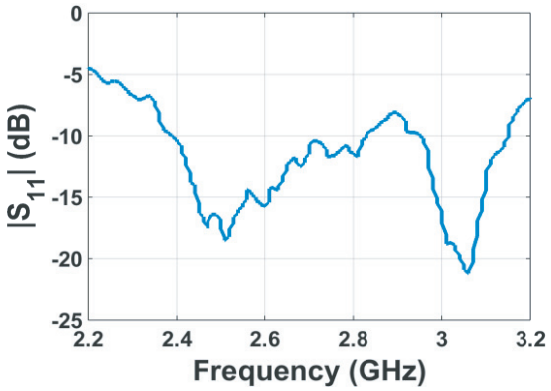

Figure 16. Measured S_{11} results vs frequency.

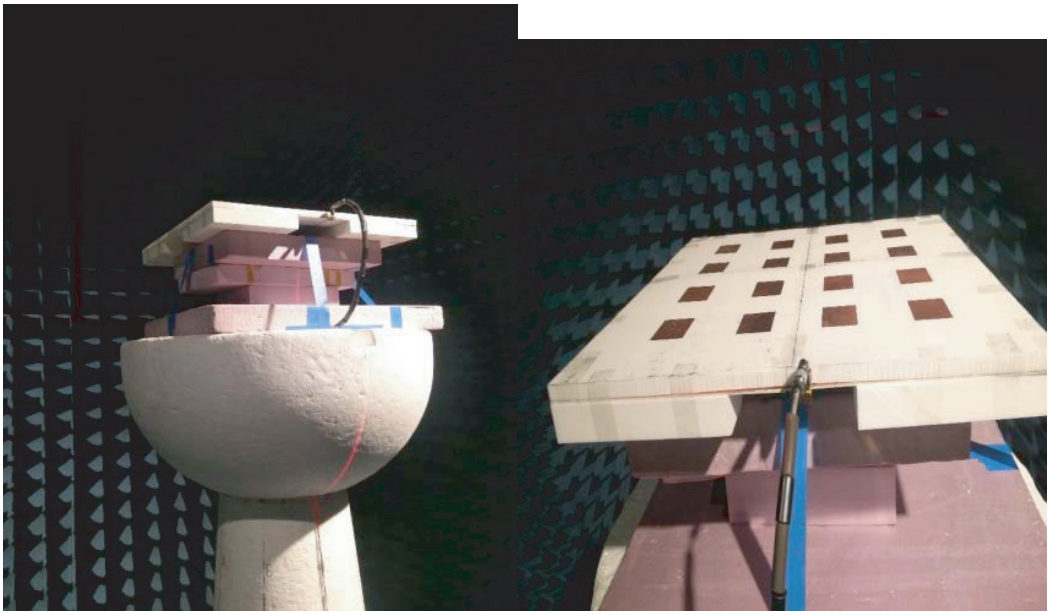

(a)

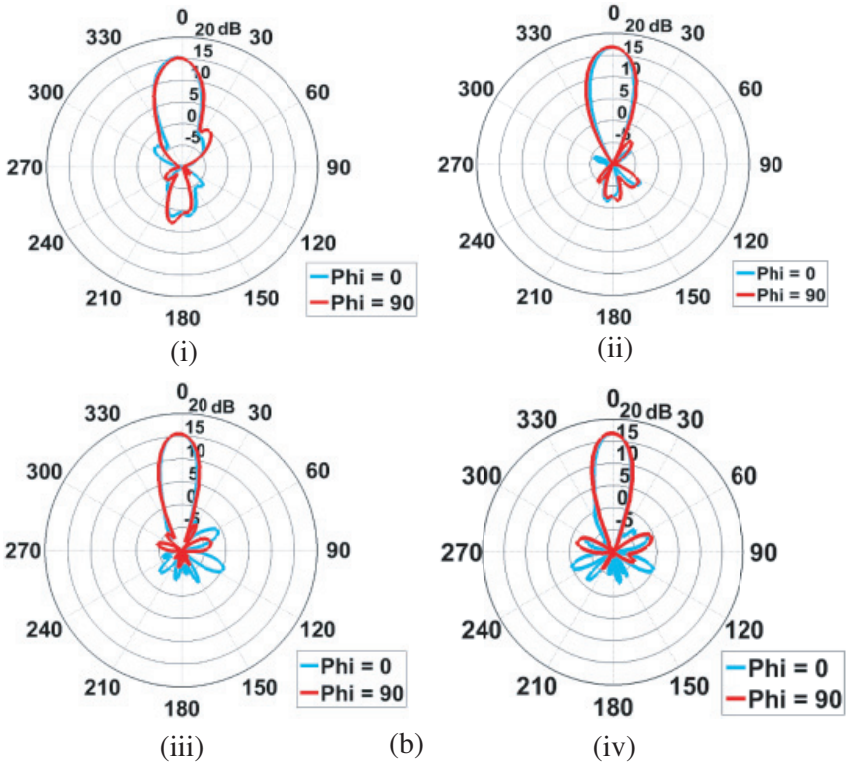

(b)

Figure 17. (a) Antenna array test setup inside Satimo anechoic chamber. (b) Measured radiation patterns at (i) 2.45, (ii) 2.65, (iii) 3, (iv) 3.1 GHz.

suggest. Surprisingly though, the F/B is much better than the simulations. The measurement setup in the anechoic chamber is such that the region right under the pedestal cannot be measured. To be precise a total angle of 23.6° lies in this blind spot. The software uses a predictive algorithm to estimate the radiation pattern in this region based on various factors like the magnitude of the radiation pattern right before the blind spot, the rate of change, etc. and extrapolates on the basis of these data.

Table 5. Measured gain, SLL and F/B Data for 4 by 4 array.

Frequency (GHz)	Array Directivity (dBi)	Realized Gain (dBi)	SLL (dB)	F/B (dB)
2.45	17.4	15.4	15.3	14.7
2.65	19	16.8	20.7	19.4
3	18.9	15.7	16.5	22.9
3.1	19.6	16.8	17.6	25.4

4.4. Corporate Fed Low Side Lobe 4 by 4 Array with Reflector

4.4.1. Simulation Results

To understand and evaluate the effects of a metal reflector behind the feed substrate parametric simulations were performed by placing a reflector at height, h_r from the feed substrate. The stackup is shown in Fig. 18(a). Simulated S_{11} results for various values of h_r are shown in Fig. 18(b). It is apparent that for most of the h_r values S_{11} performance is good. Clearly $h_r = 25\,\text{mm}$ provides the best performance. Simulated radiation patterns for various h_r values are plotted in Fig. 19. Again, $h_r = 25\,\text{mm}$ appears to provide the widest bandwidth performance among the values considered. All pattern related parameters for this case are listed in Table 6.

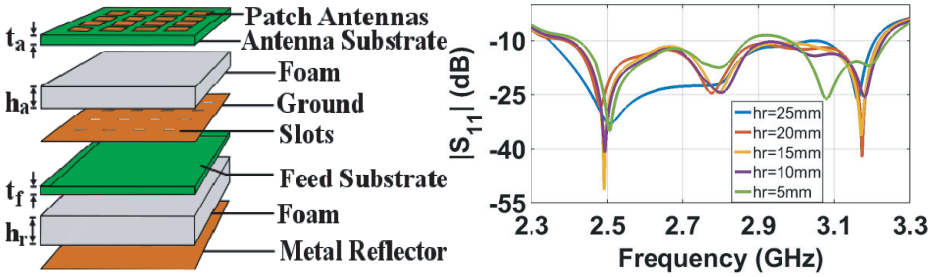

(a) (b)

Figure 18. Cross-sectional view of array with the reflector.

Table 6. Simulation data for the 4 by 4 array with metal reflector.

Frequency (GHz)	Realized Gain (dBi)	SLL (dB)	F/B (dB)
2.45	17.4	20.4	21.8
2.65	18. 7	18.9	19.8
3	19.6	12.9	14.4
3.1	18.9	12.3	14.8

4.4.2. Experimental Results

Measured S_{11} vs frequency results for the array with the reflector at $h_r = 25\,\text{mm}$ are shown in Fig. 20. The array operates from 2.4 to 3.15 GHz except within the frequency range of 2.7 to 3 GHz the S_{11} exceeds $-10\,\text{dB}$. The placement of the reflector somewhat degraded the S_{11} compared to the one shown without it (see Fig. 16). Nevertheless, the S_{11} was better than $-8.2\,\text{dB}$ (VSWR < 2.5) throughout the band. Subsequently the array was measured for pattern and gain (Fig. 21).

Measured patterns of the array with the reflector are shown in Fig. 21. Clearly the patterns are highly directional and the F/B is very high. Measured realized gain, SLL, and F/B data are listed in Table 7. Realized gain is between 16.2 and 17.5 dBi while SLL is between 13.4 and 19.2 dB.

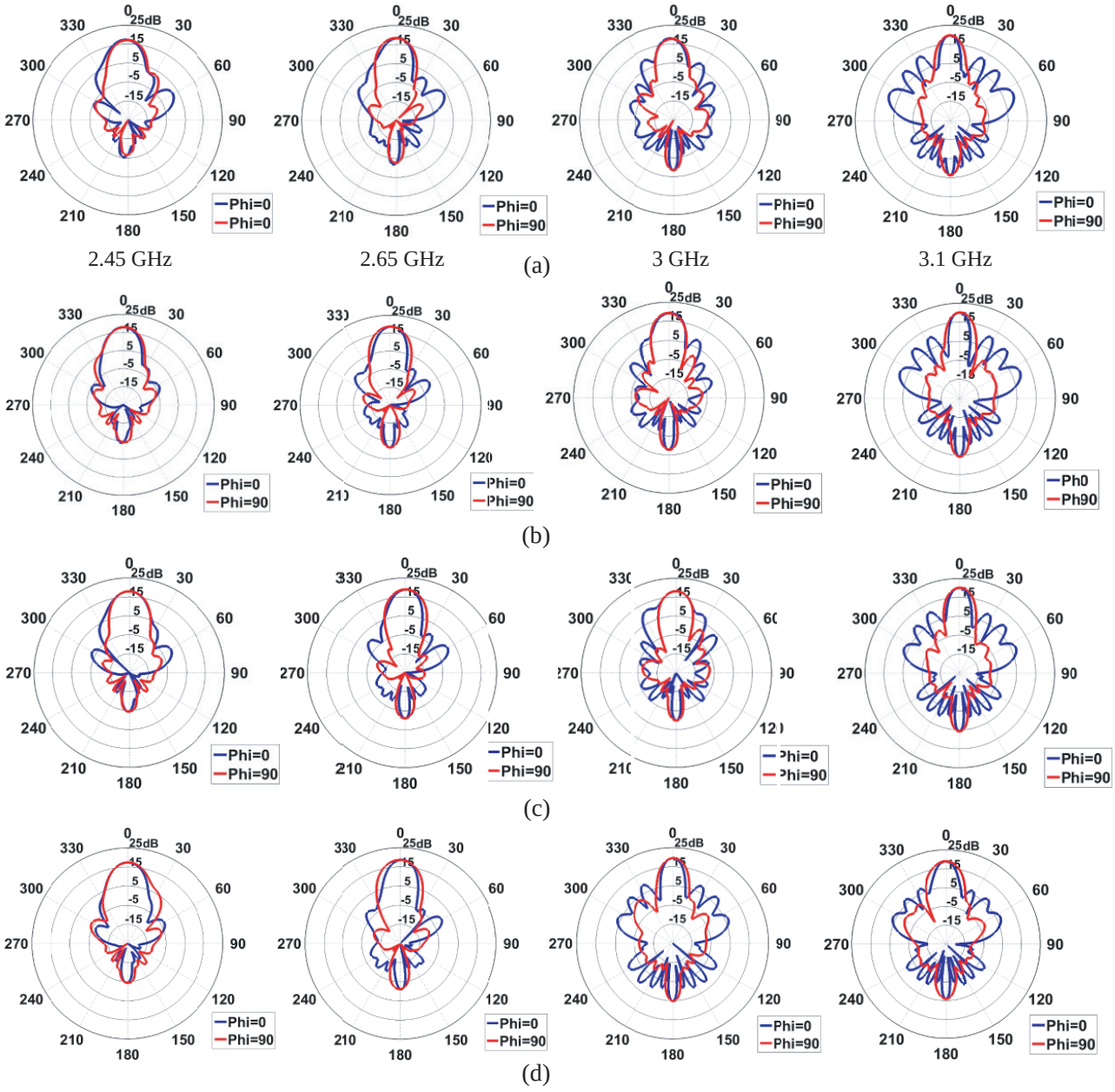

Figure 19. Simulated radiation pattern plots with reflector at different heights. (a) $h = 10\,\text{mm}$ $(0.08\lambda_0)$, (b) $h = 15\,\text{mm}$ $(0.12\lambda_0)$, (c) $h = 20\,\text{mm}$ $0.16\lambda_0$, (d) $h = 25\,\text{mm}$ $(0.204\lambda_0)$.

Table 7. Measured data for 4 by 4 array with reflector.

Frequency (GHz)	Array Directivity (dBi)	Realized Gain (dBi)	SLL (dB)	F/B (dB)
2.45	17.9	16.2	15.2	37.1
2.65	19.4	17.5	19.2	43.3
3	20	17.2	15.3	38.7
3.1	19.3	16.4	13.4	37.2

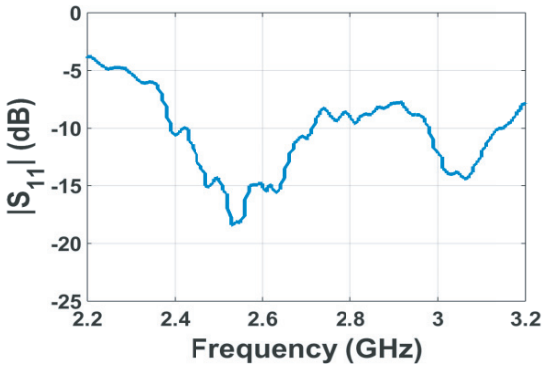

Figure 20. Measured S_{11} results for array with reflector.

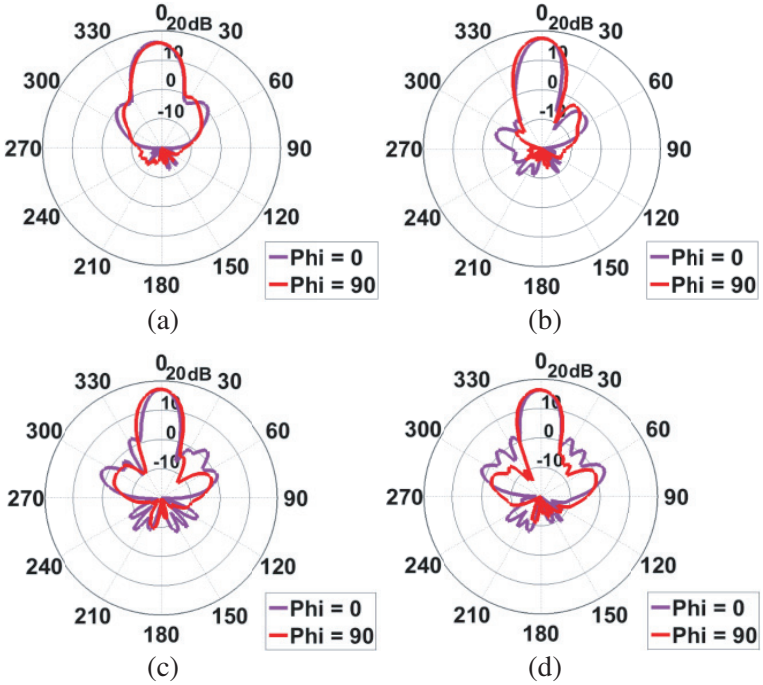

Figure 21. Measured radiation pattern plots for array with reflector at (a) 2.45, (b) 2.65, (c) 3, (d) 3.1 GHz.

Table 8. Simulated and measured results side by side.

	No reflector				With reflector			
Freq (GHz)	Gain (Sim.)	Gain (meas.)	SLL (SIM.)	SLL (Meas.)	Gain (Sim.)	Gain (meas.)	SLL (SIM.)	SLL (Meas.)
2.45	17.2	15.4	25.5	15.3	17.4	16.2	20.4	15.2
2.65	18.6	16.8	27.2	20.7	18.7	17.5	18.9	19.2
2.85	18.6	15.7	18.5	16.5	19.6	17.2	12.9	15.3
3.05	18.6	16.8	18.6	17.6	18.9	16.4	12.3	13.4

4.4.3. Comparison and Discussion

Comparisons between simulated and measured results of gain and SLL are performed in Tables 8 and 9. The disagreement between the simulated and measured results may be explained from the

Table 9. Difference between simulated and measured results.

	No reflector		With reflector	
Freq (GHz)	$\Delta\text{Gain}\vert_{\text{Sim-Meas}}$	$\Delta SLL\vert_{\text{Sim-Meas}}$	$\Delta\text{Gain}\vert_{\text{Sim-Meas}}$	$\Delta SLL\vert_{\text{Sim-Meas}}$
2.45	1.8	10.2	1.2	5.2
2.65	1.8	6.5	1.2	−0.3
2.85	2.9	2	2.4	−3.4
3.05	1.8	1	2.5	−1.1

Table 10. Comparison between the gain, SLL, and F/B considering with and without reflector (Simulated data).

Freq (GHz)	$\Delta\text{Gain}\vert_{\text{Re-No Re}}$	$\Delta SLL\vert_{\text{Re-No Re}}$	$\Delta F/B\vert_{\text{Re-No Re}}$
2.45	0.2	−5.1	12.5
2.65	0.1	−8.3	4.6
2.85	1.0	−5.6	2.7
3.05	0.3	−6.3	2.5

fabrication and alignment imperfections and substrate material properties and thickness variations. When comparing between reflector and no reflector (Table 10) it is clear that the primary benefit the reflector provides is an increase in the F/B but at the expense of higher SLL. The effect of the reflector on the gain is modest.

5. CONCLUSION

The analysis and design of a 2.4 to 3 GHz wideband aperture coupled microstrip patch array is presented. Starting from a basic elemental patch design the mutual coupling between the elements is studied by feeding each individual patch separately. The array design started with a half wavelength inter-element distance at 2.45 GHz. This ensured that the inter-element distance is less than 0.65 wavelength even at the highest frequency. However, a corporate feed design that was adopted showed the limitations of the feed layout. The feed layout caused undesired coupling between the lines that are adjacent to each other. This was corrected by increasing the inter-element spacing between the elements to 0.68 wavelength at 2.45 GHz. This was done by examining the field distributions on the feedline and the apertures. Note that the increased spacing is not the only way to solve the problem with the corporate fed array that was attempted. Another way would be to instead use a smaller inter-element spacing such as 0.5 wavelength and make the spacings between the feedlines and the slots symmetric by meandering the feedlines so that their associated electrical delays are the same. The tapered feedline was designed such that 25 dB SLL could be obtained at 2.45 GHz. The highest SLL obtained in simulations was 27.2 dB while the highest SLL obtained in measurement was 20.7 dB. The measured SLL was somewhat lower due to fabrication errors as explained above. Measured gain was from 15.4 to 16.8 dBi and measured SLL was from 15.3 to 20.7 dB without a reflector. With a reflector significant increase in F/B is obtained but at the expense of lower SLL. The design and the results presented here could be used as a guide to further develop patch array and likely planar patch phased arrays with wideband characteristics. For phased array development, more work will be needed to determine optimum inter-element spacing and feed and phase shifter design.

REFERENCES

1. Munson, R. E., "Conformal microstrip antennas and microstrip phased arrays," *IEEE Trans. Antennas and Propagat.*, Vol. 22, No. 1, 74–78, Jan. 1974.

2. Pozar, D. M., "Microstrip antennas," *Proceedings of the IEEE*, Vol. 80, No. 1, 79–91, Jan. 1992.
3. Yang, F., X. X. Zhang, X. Ye, and Y. Rahmat-Samii, "Wide-band E-shaped patch antennas for wireless communications," *IEEE Trans. Antennas and Propagat.*, Vol. 49, 1094—1100, Jul. 2001.
4. Chair, R., C. L. Mak, K. F. Lee, K. M. Luk, and A. A. Kishk, "Miniature wide-band half U-slot and half E-shaped patch antennas," *IEEE Trans. Antennas and Propagat.*, Vol. 53, 2645–2652, Aug. 2005.
5. Wang, H., X. B. Huang, and D. G. Fang, "A single layer wideband U-slot microstrip patch antenna array," *IEEE Antennas and Wireless Propagat. Letters*, Vol. 7, 9–12, 2008.
6. Lam, K. Y., K. M. Luk, K. F. Lee, H. Wong, and K. B. Ng, "Small circularly polarized U-slot wideband patch antenna," *IEEE Antennas and Wireless Propagat. Letters*, Vol. 10, 87–90, 2011.
7. Wang, S., H. W. Lai, K. K. So, K. B. Ng, Q. Xue, and G. Liao, "Wideband shorted patch antenna with a modified half U-slot," *IEEE Antennas and Wireless Propagat. Letters*, Vol. 11, 689–692, 2012.
8. Liu, S., W. Wu, and D. G. Fang, "Single-feed dual-layer dual-band E-shaped and U-slot patch antenna for wireless communication application," *IEEE Antennas and Wireless Propagat. Letters*, Vol. 15, 468–471, 2016.
9. Ali, M., A. T. M. Sayem, and V. K. Kunda, "A reconfigurable stacked microstrip patch antenna for satellite and terrestrial links," *IEEE Trans. Vehicular Technology*, Vol. 56, 426–435, Mar. 2007.
10. Splitt, G., "Guidelines for design of electromagnetically coupled microstrip patch antennas on two-layer substrates," *IEEE Trans. Antennas and Propagat.*, Vol. 38, No. 7, 1136–1140, Jul. 1990.
11. Pozar, D. M., "A microstrip antenna aperture coupled to a microstrip line," *Electron. Lett.*, Vol. 21, 49–50, Jan. 17, 1985.
12. Targonski, S. D., R. B. Waterhouse, and D. M. Pozar, "Wide-band aperture-coupled stacked patch antenna using thick substrate," *Electron. Lett.*, Vol. 32, No. 21, 1941–1942, Nov. 1996.
13. Poduval, D. and M. Ali, "A broadband high-gain aperture coupled patch array for communication and radar applications," *IEEE Antennas and Propagation Society International Symposium*, San Diego, Jul. 2017.
14. Balanis, A., *Antenna Theory: Analysis and Design*, 3rd Edition, John Wiley and Sons, Inc., Hoboken, New Jersey, 2005.
15. Pozar, D. M., *Microwave Engineering*, 4th Edition, John Wiley and Sons, Inc., Hoboken, New Jersey, 2012.
16. Keizer, W. P. M. N., "Fast low side-lobe synthesis for large planar array antennas utilizing successive fast Fourier transforms of the array factor," *IEEE Trans. Antennas and Propagat.*, Vol. 55, No. 3, 715—722, Mar. 2007.
17. Keizer, W. P. M. N., "Element failure correction for a large monopulse phased array antenna with active amplitude weighting," *IEEE Trans. Antennas and Propagat.*, Vol. 55, No. 8, 2211–2218, Aug. 2007.